Available online at www.sciencedirect.com

ScienceDirect

journal homepage: www.elsevier.com/locate/he

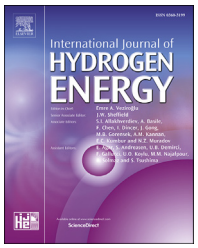

Multi-mode hydrogen storage in nanocontainers

Suboohi Shervani [a], *Puspal Mukherjee* [b], *Anshul Gupta* [a], *Gargi Mishra* [c], *Kavya Illath* [d], *T.G. Ajithkumar* [d], *Sri Sivakumar* [c], *Pratik Sen* [b], *Kantesh Balani* [a], *Anandh Subramaniam* [a,*]

[a] *Department of Materials Science and Engineering, Indian Institute of Technology, Kanpur 208016, India*
[b] *Department of Chemistry, Indian Institute of Technology, Kanpur 208016, India*
[c] *Department of Chemical Engineering, Indian Institute of Technology, Kanpur 208016, India*
[d] *Central NMR Facility, CSIR-National Chemical Laboratory, Pune 411 008, India*

ARTICLE INFO

Article history:
Received 30 May 2017
Received in revised form
28 July 2017
Accepted 29 July 2017
Available online 18 August 2017

Keywords:
Nano-containers
Hydrogen storage
Raman spectroscopy
Pressure composition isotherms
Nuclear magnetic resonance

ABSTRACT

Hydrogen can be stored in containers or in materials (in molecular or atomic forms). The atomic form can further exist as multiple phases. Molecular hydrogen can be adsorbed on the surface or can be present inside the material. By invoking multiple modes of hydrogen storage, we establish a paradigm shift in the philosophy of hydrogen storage. Using a novel strategy of storage of molecular hydrogen in metal (Pd) nanocontainers, we observe that 18% hydrogen is in molecular form. Interestingly, this is achieved at 25 °C and 1 atm pressure; which is in contrast to storage in MOFs and carbonaceous materials like nanotubes. Enhancement in storage capacity as compared to Pd nanocrystals of the same mass is observed (36% increase at 1 atm & 25 °C), along with fast kinetics (0.5 wt% hydrogen absorption in 5 s). A new mechanism for hydrogen storage involving the dual catalytic role of Pd is established.

Introduction

Hydrogen holds considerable promise as a fuel of the future [1,2]. In the utilization of hydrogen as a fuel, its storage and release are important steps [3]. Hydrogen in materials can exist in multiple forms: in molecular form (as free molecules in containers or adsorbed on the surface of materials) or in the atomic form in a host lattice. Storage of hydrogen in materials has attracted considerable attention in the past few decades and multiple classes of materials have been investigated in this regard. These include metals and alloys [4], zeolites [5], metal organic frameworks (MOFs) [6], clathrates [7] and carbonaceous materials [8,9]. Typically each of these materials stores hydrogen in one or two states/phases; e.g., in metals, it is stored as one or two solid solutions or as a solid solution and a hydride (compound) and in MOFs, it is stored in entrapped molecular form (inside the material) [10]. A specific class of these materials can offer us certain benefits in terms of hydrogen storage but correspondingly may suffer from some other lacunae. Magnesium has good storage capacity, but high temperatures are required for storage [11,12]. Carbonaceous materials can also offer good storage, but usually at low temperatures (liquid nitrogen) [13,14]. Hybrids are emerging as an important class of materials, wherein the synergistic benefits of two or more components can lead to better hydrogen storage properties [15–19].

Nanoscale materials are a natural choice as hydrogen storage materials, due to fast kinetics of absorption and

* *Corresponding author.*
E-mail address: anandh@iitk.ac.in (A. Subramaniam).
http://dx.doi.org/10.1016/j.ijhydene.2017.07.233

desorption and enhanced surface and sub-surface storage of hydrogen [20]. Nanostructured materials developed for hydrogen storage include: carbonaceous materials [13,21] (e.g. carbon nanotubes, carbon nanofibers & graphene), nanoparticles (e.g. Mg [22], Pd [23], Pt [24]), nanostructured bulk materials (e.g. ZK60 Mg Alloys [25]) and nanohybrids (e.g. Pd@MOF [26], Pd@Pt [27]). Molecular cages have also been used to store hydrogen [28]. Hollow nanospheres have been investigated in diverse contexts [29–31], including that for hydrogen storage [32,33]. Further, in a very recent article, the importance of Pd hollow spheres for hydrogen storage is highlighted using molecular dynamics [34].

In the current work, we demonstrate a novel strategy to store hydrogen in multiple modes: (i) in a container, (ii) in a material in (a) atomic form as a solid solution(s) & (b) molecular form on the surface (adsorbed). It is to be noted that the current work is a 'proof of concept' and the primary goal is not high storage capacities. This multi-pronged strategy can be exploited in the future for designing materials with highly enhanced hydrogen storage capacity, with the benefits of the fast kinetics of absorption and desorption.

Experimental details

The experimental methodology is briefly described here and the reader may refer to the Supplementary material (Section 1) for further details. To achieve the above-mentioned aims, nanoscale Pd hollow spheres (PdHS) were synthesized by first producing silica nanospheres (solid core with mesoporous shell, SCMS) [35], followed by the formation of a Pd shell using chemical reduction (sample-A1). The inner silica core was etched out by sodium hydroxide to give a porous PdHS (sample-A2). The porous PdHS (sample-A2) was evacuated at 80 °C for 12 h, followed by annealing at 200 °C to seal the pores and to obtain a non-porous PdHS (sample-A3).

Two strategies were used to 'entrap' molecular hydrogen in the nanocontainers. (A) Sample-A2: evacuation → pressurization with hydrogen → annealing to seal the pores (leading to the sample designated as A2b). (B) Sample-A3: evacuation → annealing of pores → pressurization with hydrogen (leading to the sample designated as A3b). Treatment (A) is expected to fill hydrogen in the PdHS *via* the pores followed by the sealing of the pores; while in (B), hydrogen has to be transported to the hollow core *via* the solid Pd shell. After evacuation (80 °C, 12 h & 10^{-8} atm), sample A1 is also hydrogenated at 20 atm pressure for 12 h at 200 °C to give sample A1b, which is used as a reference sample in Raman spectroscopy studies.

Pressure-composition isotherms (PCI) were obtained using a Sieverts apparatus, wherein the pressure of hydrogen was increased from 10^{-3} atm–1 atm (at 25 °C) and the amount of hydrogen absorbed by the material was measured. Two kinds of samples were tested in the PCI apparatus: (a) Pd with SiO_2 core (sample-A1) and (b) non-porous PdHS (sample-A3). The samples were activated in the PCI instrument by annealing at 300 °C for 6 h at 10^{-8} atm, followed by subjecting the samples to two cycles of absorption and desorption (akin to the practice for Pd nanoparticles [36]).

X-ray diffraction measurements of PdHS samples (samples-A1, A2, & A3) were performed using PANalytical Empyrean equipment. The measurement parameters are: (i) 2θ range of 35°–130°, (ii) step size of 0.015°, (iii) dwell time of 200 s per step and (iv) Cu Kα radiation. The scan range was limited from 35° to 85° with improved scan time (400 s per step) for the hydrogenated samples (samples-A2b & A3b). The x-ray source was operated at 45 kV and 40 mA. Lattice parameters and phase fractions were determined using the Whole Profile Fitting (also known as Pawley method, the basis of the Rietveld method) feature of JADE software supplied by Materials Data Incorporated (MDI) [37].

TEM studies were performed using FEI Technai 20 U-twin instrument operated at 200 kV. Sample-A1 & Sample-A2 were prepared using 10 mg of sample dispersed in 2 ml ethanol using ultrasonication for 30 min. The above-mentioned samples were deposited on carbon-coated Cu grids of 300 mesh size (Ted Pella, Inc. USA). The size and shape of the particle were observed using bright field images (BFI), while selected area diffraction pattern (SADP) was obtained to investigate the crystalline nature of the sample.

Raman spectroscopy was performed using high-resolution confocal micro-Raman spectrometer (STR-300) with spectral resolution less than 0.5 cm^{-1} and equipped with a cooled CCD camera. The focal length of the spectrometer is 300 mm and He-Ne LASER of the wavelength of 633 nm was used in the studies. Data were obtained in the range 3000–5000 cm^{-1} (using a grating having groove density of 600 per mm). Room temperature was maintained at 18 °C during the measurements. About 500 mg of sample was spread across a 2 mm cross-sectional area of a glass slide and this was exposed to the LASER radiation for 30 s in each accumulation. A total of 30 such data accumulations were obtained per sample. To identify the origin of the peaks in the experimental Raman spectrum, computation of Raman spectrum was performed using the Gaussian-09 software [38].

Solid-State ^1H NMR studies were performed using Bruker NMR spectrometer (700 MHz & 300 MHz), using a 1.3 mm & 4 mm MAS probe for the 700 MHz & 300 MHz frequencies respectively. Both the spectra were recorded without spinning the sample. ^1H NMR shifts were measured in parts per million (ppm), downfield from the trimethylsilane (TMS) standard sample. The samples were placed in 1.3 mm OD Zirconia rotors. In addition, hydrogenated bulk palladium sample was used as a reference for comparison with the A2b sample. In this sample, unlike the A2b sample, there is no void space for hydrogen molecules to accumulate. NMR experiments (300 MHz) were performed on sample A2b at 303 K and 328 K. For this experiment, the sample was packed into a 4 mm OD Zirconia rotor. It is to be noted that all samples were handled in a glove box (after synthesis and during transfer) to prevent hydrogen desorption, contamination and oxidation.

Results and discussions

Fig. 1 shows TEM micrographs obtained from sample-A1 and sample-A2. Inset to Fig. 1b shows the selected area diffraction pattern (SADP) obtained from sample-A2. The porous nature of the shell is to be noted and the rings indicate the nano-polycrystalline nature of the Pd shell.

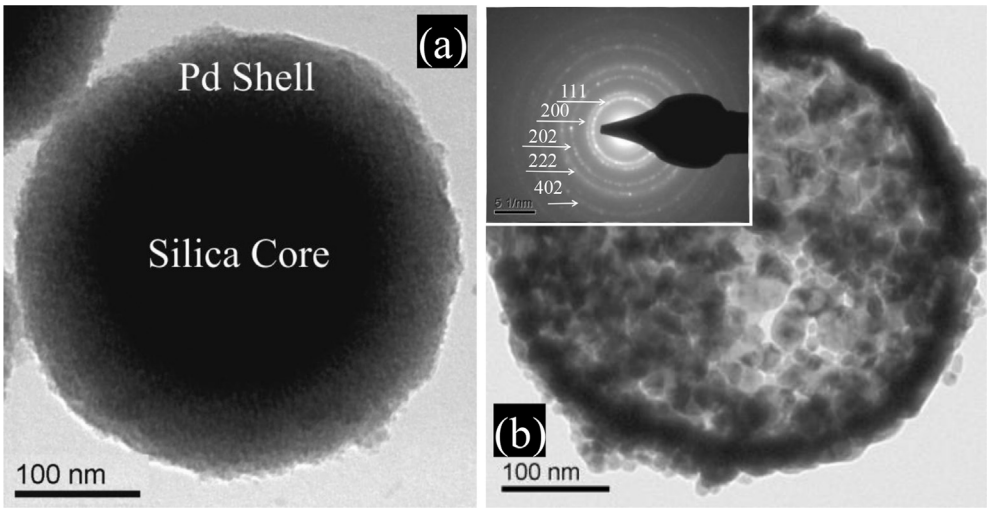

Fig. 1 – TEM bright field images of: (a) SiO_2@Pd (sample-A1) and (b) Pd hollow sphere (PdHS, sample-A2). Inset to (b) is the selected area diffraction pattern obtained from PdHS (the ring pattern shows the polycrystalline nature of the shell).

Fig. 2 shows pressure composition isotherms and kinetic curves (wt.% vs time). The weight percent in these figures is calculated as: [(wt. of hydrogen absorbed) × 100]/[(weight of (Pd + Hydrogen)]. Sample-A3 stores a higher weight percent of hydrogen (of 0.61%) as compared to sample-A1 (0.50%). The mass of Pd is identical in both the samples (hollow versus filled) and hence the additional hydrogen stored (of 0.11 wt%) must be inside the nanocontainer. This leads to an enhancement in hydrogen storage capacity of 36% over nanoparticles of the same mass, along with a decrease in plateau pressure. This amount of 0.61 wt% hydrogen absorbed is a conservative value obtained from five PCI plots. The range obtained is 0.61–0.64 wt% at 1 atm pressure (further details can be found in the supplementary material). A comparison of PCI data obtained from sample-A1 (Fig. 2a) with Pd nanoparticles shows that; (i) sample-A1 stores more hydrogen than Pd nanoparticles (of 0.45 wt%, ~7 nm [23]) and (ii) the plateau in the case of sample-A1 is nearly flat (as compared to the 'sloping plateau' for nanoparticles). The enhanced storage in sample-A1 may be attributed to the presence of two interfaces, which provide more sub-interface regions for storage of hydrogen [27,39]. Details regarding surface area measurement can be found in supplementary material. Inset in Fig. 2 shows the fast kinetics of absorption observed in sample-A3

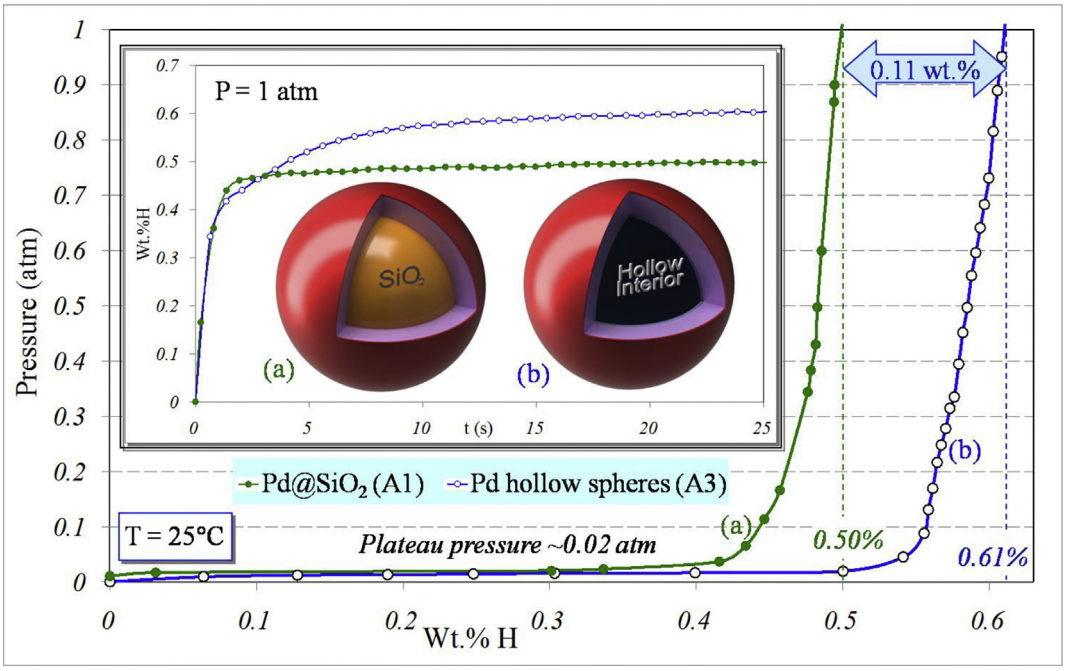

Fig. 2 – PCI curves obtained from: (a) Pd filled with SiO_2 core (sample-A1) and (b) non-porous PdHS samples (sample-A3). The inset shows kinetic measurements (wt.% hydrogen absorbed with time). The additional 0.11 wt% of hydrogen is inside the hollow sphere.

(0.5 wt% hydrogen absorbed in 5 s at 25 °C and 1 atm pressure), which is better than that observed in Pd nanoparticles under similar conditions [40].

Fig. 3 shows the XRD results from sample-A2b hydrogenated to: (a) 1 atm and (b) 0.02 atm. The formation of a single phase β interstitial solid solution of hydrogen in Pd crystal is seen in Fig. 3a, while a mixture of α & β solid solution phases is seen in (b). It is reported in nanoscale Pd that the hydrogen in the α-phase is present in the octahedral voids; while in the β-phase, 30% of the hydrogen is present in the tetrahedral voids [41]. Thus we observe that hydrogen in atomic form can be stored in more than one phase, with specific differences in the type of void involved. The lattice parameters of the α and β phases were determined to be 3.893 Å and 4.023 Å respectively and the corresponding phase fractions are 77 wt% and 23 wt% (Fig. 3b). The lattice parameter of the α-phase is slightly expanded as compared to pure PdHS (with a_{PdHS} = 3.890 Å). Details of calculations can be found in Supplementary material (Section 2.1).

Raman spectroscopy results from samples-A2b & A3b are shown in Fig. 4. The Raman signature of molecular hydrogen was analyzed using three kinds of models: (i) free molecular hydrogen, (ii) hydrogen adsorbed on crystalline surfaces ((111), (110) & (100) surfaces of Pd & $PdH_{0.54}$) and (iii) weakly adsorbed hydrogen (as in second and higher layers in multi-layer adsorbates). The details of the computation along with the models used can be found in the Supplementary material (Section 1.7.1). The results of the computations are overlaid on Fig. 4 as vertical dashed lines. A combined view of the experimental and computational data shows the existence of molecular hydrogen in three forms: (i) free, (ii) adsorbed on Pd surface and (iii) bi/multi-layer adsorbate. It is interesting to note that in spite of the complications arising from the myriad of possibilities with respect to the adsorption of hydrogen [42] (crystallography of the surface, surface ledges/kinks, surface curvature, etc.), sharp Raman peaks are obtained [43]. A comparison of the Raman spectra of sample-A1b with that from samples-A2b & A3b (Fig. 4) shows the absence of molecular hydrogen in the sample with SiO_2 core. Given that diffusion of atomic hydrogen through the hydride is sluggish, it is expected that lesser amount of molecular hydrogen is entrapped inside sample-A3b (along with a lesser amount of adsorbed H_2). Detailed discussions can be found in the Supplementary material (Section 2.4).

To unequivocally establish the existence of molecular hydrogen in the nanocontainer, a nuclear magnetic resonance (^{1}H solid-state static NMR) study was carried out to augment the Raman experiments. Sample-A2b gives a sharp and intense peak as compared to hydrogenated bulk Pd, which gives a broad peak (inset to Fig. 4). The existence of the sharp peak corroborates well with the signature of molecular hydrogen [44], thus firmly establishing our confidence in the presence of the same. Details related to NMR spectroscopy are considered in the Supplementary material (Section 2.3).

In sample-A1 (with SiO_2 inside the Pd shell) the hydrogen is absorbed in the Pd shell only, as the silica core is expected to accommodate negligible amounts of hydrogen; while in non-porous PdHS hydrogen can be stored both in the shell (atomic form) and in the interior of the Pd shell (container) in molecular form. Thus, combining the PCI and Raman data, we can now conclude that the additional hydrogen absorbed (0.11 wt%) in sample-A3b is in the form of molecular hydrogen trapped inside the PdHS. As noted before, the Raman spectra show that molecular hydrogen is in both free and adsorbed forms in sample-A2b (& A3b).

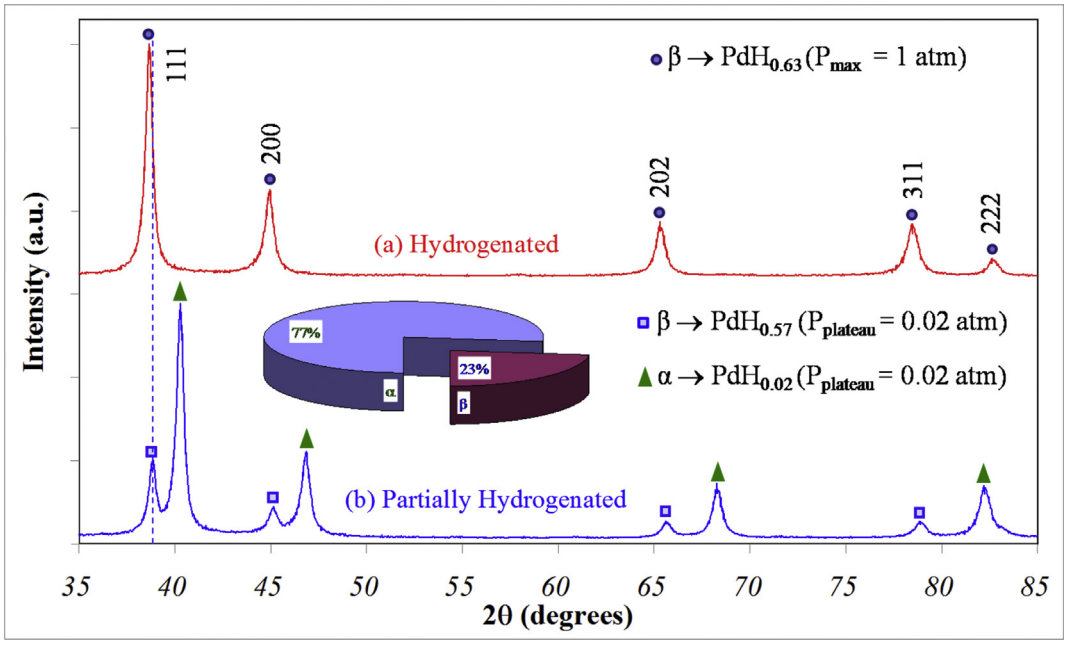

Fig. 3 – XRD patterns from PdHS samples (sample-A3) hydrogenated to a pressure of: (a) 1 atm, (b) 0.02 atm. The stoichiometry of the β-phase obtained in the two cases are: $PdH_{0.63}$ & $PdH_{0.57}$ respectively. The vertical dotted line shows the shift in the position of the 111 peak. Inset to (b) shows the phase fractions of α and β phases. The presence of atomic hydrogen in multiple phases is established (in b).

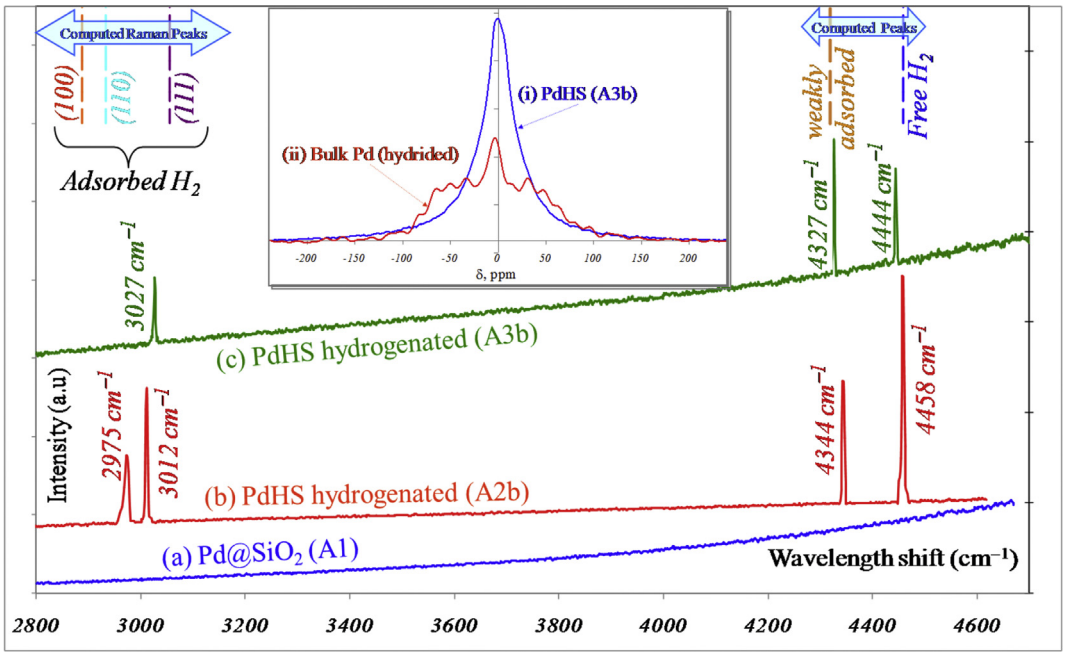

Fig. 4 – Raman spectra obtained from the following samples: (a) Pd filled with SiO_2 core (A1b), (b) A2b, (c) A3b. Peak positions computed using Gaussian software is overlaid on the plots (dashed vertical lines at the top). Complete computed spectra can be found in the Supplementary material (Section 2.2). The inset shows ^{1}H solid state static NMR spectra obtained from: (i) sample-A2b and (ii) hydrogenated bulk Pd. The presence of molecular hydrogen in free form, adsorbed on metal and as bi/multi-layer adsorbate is confirmed.

The difference in the mechanism of entrapping molecular hydrogen between samples-A2 & A3 (leading to samples-A2b & A3b) is to be noted. In sample-A2 hydrogen is filled in *via* the pores and the pores are subsequently sealed to trap the hydrogen molecules. In sample-A3, physisorbed H_2 first dissociates into atomic H at the surface of Pd (gets chemisorbed), followed by its diffusion across the Pd shell (inward). Further, the hydrogen atoms recombine at the inner surface of the PdHS to form the H_2 molecule (Fig. 5). This shows that the internal pressure in Sample-A2 and Sample-A3 are considerably different. The pressure inside sample-A3 builds up *via* diffusion of hydrogen and further recombination. Some of the molecular hydrogen present in the PdHS samples is in the form of adsorbed molecules. These aspects imply that the internal pressure of hydrogen in sample-A3 could be much lower than the hydrogenation pressure in the chamber.

In sample-A3b the molecular hydrogen is about 18% of the total hydrogen stored. Given that the absorption studies have been carried out at 25 °C, a comparison with materials like carbon nanotubes and MOFs is noteworthy. In these materials, low temperatures (77 K) and/or high pressures (>50 atm) are required for the storage of molecular hydrogen [13]. In any case, in none of these materials is the hydrogen present in both free and adsorbed forms. Some of the observations of the current experimental study corroborate well with the computational work of Valencia et al. [34]; however, their conceptualization and configurations are considerably different. Combining the results of Fig. 2 (0.11 wt% H_2 is inside the container) and Fig. 4c we can make the following 'curious' observations: (i) the Sieverts apparatus has been utilized for 'molecular spectroscopy' ('detection' of molecular hydrogen) and (ii) Pd is performing a double catalytic role (breaking of H_2

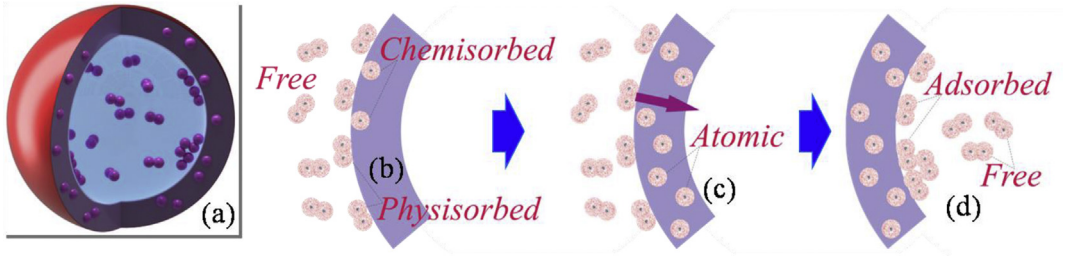

Fig. 5 – Schematic showing the mechanism by which hydrogen molecules are trapped inside PdHS sample-A3b (a). The steps involved are: (b) physisorption & chemisorption, (c) diffusion, (d) recombination and 'de-adsorption'. The 'dual' catalytic role of Pd is to be noted.

into H + H on the outer surface and recombination of atomic hydrogen on the inner surface to form H_2).

Summary and conclusions

We can summarize the current investigation as follows. Hydrogen can be stored in containers or in materials. In materials, it can exist in molecular or atomic forms. The atomic form can further exist as multiple phases. Molecular hydrogen can be adsorbed on the surface or can be present inside the material. In the current work we have developed a novel methodology to store hydrogen in multiple modes (akin to a 'Swiss knife'): in a container, in molecular (adsorbed and free) and atomic (α & β solid solutions) forms. Further, the adsorbed hydrogen is demonstrated to be in single and multiple layers. More than one method is developed to store hydrogen in molecular form, with an interesting mechanism of dissociation and recombination of hydrogen molecule being operative in non-porous PdHS samples; wherein Pd performs a *'double catalytic'* role. This strategy leads to a considerable enhancement in the capacity as compared to Pd nanoparticles of the same mass (36% increase at 1 atm, 25 °C), along with fast kinetics (0.5 wt% absorption in 5 s). Further, this is the first instance of storage of free molecular hydrogen in metallic nanocontainers. Molecular hydrogen is about 18% of the total hydrogen stored and interestingly this is achieved at room temperature (25 °C) and 1 atm pressure. This is in stark contrast to materials like carbon nanotubes and MOFs, wherein low temperatures or high pressures are required for the storage of molecular hydrogen. One 'curious' highlight of the current work is the use of Sieverts apparatus for 'molecular spectroscopy' ('detection' of molecular hydrogen). Further work can take this 'proof of concept' ahead, resulting in practical materials targeting applications.

Funding

This research did not receive any specific grant from funding agencies in the public, commercial, or not-for-profit sectors.

Methods

Details regarding the methods can be found in the supplementary material.

Appendix A. Supplementary data

Supplementary data related to this article can be found at http://dx.doi.org/10.1016/j.ijhydene.2017.07.233.

REFERENCES

[1] Dresselhaus MS, Thomas IL. Alternative energy technologies. Nature 2001;414:332–7.
[2] Mohan V, Shah A, Sheffield JW, Martin KB. Design of a hydrogen community. Int J Hydrogen Energy 2012;37:1214–9.
[3] Schlapbach L, Zuttel A. Hydrogen-storage materials for mobile applications. Nature 2001;414:353–8.
[4] Cermak J, Kral L. Improvement of hydrogen storage characteristics of Mg/Mg_2Ni by alloying: beneficial effect of In. J Power Sources 2012;214:208–15.
[5] Chung KH. High-pressure hydrogen storage on microporous zeolites with varying pore properties. Energy 2010;35:2235–41.
[6] Li J, Cheng S, Zhao Q, Long P, Dong J. Synthesis and hydrogen-storage behavior of metal-organic framework MOF-5. Int J Hydrogen Energy 2009;34:1377–82.
[7] Talyzin A. Feasibility of H_2–THF–H_2O clathrate hydrates for hydrogen storage applications. Int J Hydrogen Energy 2008;33:111–5.
[8] Jena P. Materials for hydrogen storage: past, present and future. J Phys Chem Lett 2011;2:206–11.
[9] Orinakova R, Orinak A. Recent applications of carbon nanotubes in hydrogen production and storage. Fuel 2011;90:3123–40.
[10] Pukazhselvan D, Kumar V, Singh SK. High capacity hydrogen storage: basic aspects, new developments and milestones. Nano Energy 2012;1:566–89.
[11] Shao H, Xin G, Zheng J, Li X, Akiba E. Nanotechnology in Mg-based materials for hydrogen storage. Nano Energy 2012;1:590–601.
[12] Fan MQ, Liu SS, Zhang Y, Zhang J, Sun LX, Xu F. Superior hydrogen storage properties of MgH_2–10 wt% TiC composite. Energy 2010;35:3417–21.
[13] Bastos-Neto M, Patzschke C, Lange M, Mollmer J, Moller A, Fichtner S. Assessment of hydrogen storage by physisorption in porous materials. Energy Environ Sci 2012;5:8294–303.
[14] Yadav A, Faisal M, Subramaniam A, Verma N. Nickel nanoparticle-doped and steam-modified multiscale structure of carbon micro-nanofibers for hydrogen storage: effects of metal, surface texture and operating conditions. Int J Hydrogen Energy 2017;42:6104–17.
[15] Hao Y, Wang X, Bi K, Zhang J, Huang Y, Wu L, et al. Significantly enhanced energy storage performance promoted by ultimate sized ferroelectric $BaTiO_3$ fillers in nanocomposite films. Nano Energy 2017;31:49–56.
[16] Gupta A, Shervani S, Faisal M, Balani K, Subramaniam A. Hydrogen storage in Mg-Mg_2Ni-carbon hybrids. J Alloys Compd 2014;645:S397–9.
[17] Faisal M, Gupta A, Shervani S, Balani K, Subramaniam A. Enhanced hydrogen storage in accumulative roll bonded Mg-based hybrid. Int J Hydrogen Energy 2015;40:11498–505.
[18] Jeon KJ, Moon HR, Ruminski AM, Jiang B, Kisielowski C, Bardhan R, et al. Air-stable magnesium nanocomposites provide rapid and high-capacity hydrogen storage without using heavy-metal catalysts. Nat Mater 2011;10:286–90.
[19] Chen LX, Zhu YF, Yang CC, Chen ZW, Zhang DM, Jiang Q. A new strategy to improve the high-rate performance of hydrogen storage alloys with MoS_2 nanosheets. J Power Sources 2016;333:17–23.
[20] Zaluska A, Zaluski L, Ström-Olsen JO. Structure, catalysis and atomic reactions on the nano-scale: a systematic approach to metal hydrides for hydrogen storage. Appl Phys A 2001;72:157–65.
[21] Schur DV, Tarasov BP, Yu S, Pishuk VK, Veziroglu TN, Shulga YM, et al. The prospects for using of carbon nanomaterials as hydrogen storage systems. Int J Hydrogen Energy 2002;27:1063–9.
[22] Pasquini L, Brighi M, Montone A, Antisari MV, Dam B, Palmisano V. Magnesium nanoparticles for hydrogen storage: structure, kinetics and thermodynamics. IOP Conf Ser Mat Sci Eng 2012;38:012001.

[23] Yamauchi M, Ikeda R, Kitagawa H, Takata M. Nanosize effects on hydrogen storage in palladium. J Phys Chem C 2008;112:3294–9.
[24] Yamauchi M, Kobayashi H, Kitagawa H. Hydrogen storage mediated by Pd and Pt nanoparticles. Chem Phys Chem 2009;10:2566–76.
[25] Kristian M, Zehetbauer MJ, Kropik H, Mingler B, Krexner G. Hydrogen storage properties of bulk nanostructured ZK60 Mg alloy processed by equal channel angular pressing. J Alloys Compd 2011;509:S449–55.
[26] Li G, Kobayashi H, Taylor JM, Ikeda R, Kubota Y, Kato K, et al. Hydrogen storage in Pd nanocrystals covered with a metal-organic framework. Nat Mater 2014;13:802–6.
[27] Kobayashi H, Yamauchi M, Kitagawa H, Kuboto Y, Kato K, Takata M. Hydrogen absorption in the core/shell interface of Pd/Pt. J Am Chem Soc 2008;130:1818–9.
[28] Komatsu K, Murata M, Murata Y. Encapsulation of molecular hydrogen in Fullerene C_{60} by organic synthesis. Science 2005;307:238–40.
[29] Zheng G, Lee SW, Liang Z, Lee HW, Yan K, Yao H, et al. Interconnected hollow carbon nanospheres for stable lithium metal anodes. Nat Nanotechnol 2014;9:618–23.
[30] Cho JS, Lee JK, Kang YC. Graphitic carbon- coated FeS_2 hollow nanospheres- decorated reduced Graphene oxide hybrids nanofibres as an efficient anode material for sodium ion batteries. Sci Rep 2016;6:23699.
[31] Cho JS, Ju HS, Kang YC. Applying nanoscale kirkendall diffusion for template free, kilogram scale production of SnO_2 hollow nanospheres via Spray drying system. Sci Rep 2016;6:23915.
[32] Lian G, Zhang X, Zhang S, Liu D, Cui D, Wang Q. Controlled fabrication of ultrathin-shell BN hollow spheres with excellent performance in hydrogen storage and wastewater treatment. Energy Environ Sci 2012;5:7072.
[33] Kong Q, Feng W, Zhong X, Liu Y, Lian L. Hydrogen absorption/desorption properties of porous hollow palladium spheres prepared by templating method. J Alloys Compd 2016;664:188–92.
[34] Valencia FJ, Gonzalez RI, Tramontina D, Rogan J, Valdivia JA, Kiwi M, et al. Hydrogen storage in palladium hollow nanoparticles. J Phys Chem C 2016;120:23836–41.
[35] Buchel G, Unger KK, Matsumoto A. A novel pathway for synthesis of submicrometer-size solid core/mesoporous shell silica spheres. Adv Mater 1998;10:1036–8.
[36] Vons VA, Leegwater H, Legerstee WJ, Eijt SWH, Schmidt-ott A. Hydrogen storage properties of spark generated palladium nanoparticles. Int J Hydrogen Energy 2010;35:5479–89.
[37] MDI. JADE v. 2.6.3 software provided by materials data, Inc., (MDI). 2010. http://www.materialsdata.com/.
[38] Frisch MJ, Trucks GW, Schlegel HB, Scuseria GE, Robb MA, Cheeseman JR, et al. Gaussian 09, Revision B.01. Wallingford CT: Gaussian, Inc.; 2010.
[39] Ouyang LZ, Ye SY, Dong HW, Zhu M. Effect of interfacial free energy on hydriding reaction of Mg–Ni thin films. Appl Phys Lett 2007;90:021917.
[40] Liu T, Xie L, Li Y, Li X, Pang S, Zhang T. Hydrogen/deuterium storage properties of Pd nanoparticles. J Power Sources 2013;237:74–9.
[41] Akiba H, Kofu M, Kobayashi H, Kitagawa H, Ikeda K, Otomo T, et al. Nanometer-size effect on hydrogen sites in palladium lattice. J Am Chem Soc 2016;138:10238–43.
[42] Gribov EN, Bertarione S, Scarano D, Lamberti C, Spoto G, Zecchina A. Vibrational and thermodynamic properties of H_2 adsorbed on MgO in the 300-20 K interval. J Phys Chem B 2004;108:16174–86.
[43] Ouyang L, Tang J, Zhao Y, Wang H, Yao X, Liu J, et al. Express penetration of hydrogen on Mg(1013) along the closepacked-planes. Sci Rep 2015;5:10776.
[44] Senadheera L, Carla EM, Ivancica TM, Conradi MS, Bowman Jr RC, Hwang S-J, et al. Molecular hydrogen trapped in AlH_3 solid. J Alloys Compd 2008;463:1–5.